Demonstration of Electron Wave-Particle Duality Through Diffraction and Measurement of Charge/Mass Ratio

Chase Foster and Jun Chang

Two experiments were performed to demonstrate that electrons display both wave and particle properties. In the first experiment, electrons were shot through a graphite sample, and the resulting scattering produced a diffraction pattern similar to wave diffraction from an ordered crystal. The scattering data then were used to calculate the atomic spacing between the atoms in the sample and to confirm Braggs Law and deBroglies equations for electron wavelength and energy. In the second experiment, electrons were shot into a uniform magnetic field. The orbit of the electrons in the field was measured, and the charge/mass ratio of the electron was obtained over several voltages. Combined, the two experiments showed that the electron has both wave-like and particle-like behavior.

I. INTRODUCTION

For many years, physicists believed that certain physical objects displayed either exclusively wave-like or particle-like behavior. In the 19th Century, Maxwells seminal equations (Maxwell 1864) were used to predict that the behavior of light could be understood as waves caused by changes in electromagnetic fields. This discovery lead to the belief that light was a purely wave-like phenomenon. In contrast, Thompson (Thomson 1897) later demonstrated that electrons emitted by a cathode traveled through vacuum, a behavior that is not possible for mechanical waves. Thus, physicists came to believe that electrons were purely particulate matter, and they believed that wave-like and particle-like behavior would be mutually exclusive.

But with Einsteins proposition (Einstein 1965) that the photoelectric effect could be explained if light was quantized and possessed particle properties, the total distinction between wave-like and particle-like behavior was challenged. The quantization of light lead physicists to question whether, if wave phenomena such as light demonstrated particulate behavior, particles such as electrons could display wave-like behavior. Soon thereafter, de Broglie (De Broglie 1924) proposed that particulate matter would indeed demonstrate wave-like behavior under the right conditions. This proposition was tested soon after, and it fundamentally eliminated the exclusivity of wave-like or particle like behavior in matter.

In this paper, we provide evidence that electrons display both wave-like and particle-like behavior in agreement with de Broglies hypothesis. The first experiment tests the wave-like behavior of the electron via the firing of electrons into a graphite crystal, which produces a scattering pattern. The scattering data are then used to test de Broglies equation for wavelength and calculate the spacing between the carbon atoms in graphite. The second experiment verifies the particle-like behavior of the electron via the firing of electrons into a uniform magnetic field. The electrons orbit in the field, and the radius of orbit is used to calculate the charge/mass ratio of the electron, a distinctly particle-like property.

II. THEORY

De Broglie postulated that electrons would have a wavelength given by

$$\lambda = \frac{h}{p} \tag{1}$$

As electrons are fired through a potential $eV = \frac{p^2}{2m}$, the wavelength becomes

$$\lambda = \frac{h}{\sqrt{2eVm}}. \tag{2}$$

If electrons do possess wave-like properties, then they should scatter from a diffraction grating in a typical diffraction pattern. The angle of diffraction from the grating is governed by Braggs Law, which is derived from geometric arguments from the figure below:

$$2d\sin\theta = n\lambda, \tag{3}$$

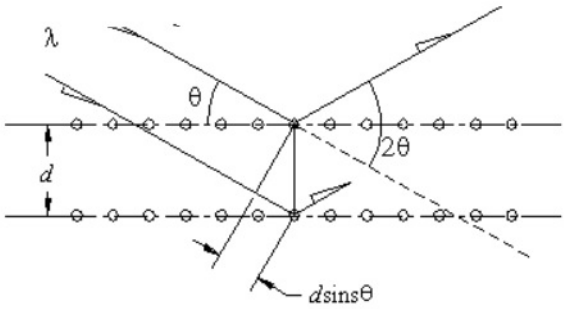

FIG. 1. Bragg's Law Geometry (retrieved from lab manual)

where n is a natural number and d is the separation between carbon atoms. In this experiment, a graphite crystal is positioned in front of incident electrons, and it acts as a diffraction grating for electron scattering. Thus, the electrons should scatter at angles in agreement with Braggs Law. Using these equations, we eliminate θ to find

$$\sin\theta = \frac{h}{d\sqrt{8me}}\frac{1}{\sqrt{V}}, \tag{4}$$

where d is the spacing between layers of the grating, which are the carbon atoms in the graphite crystal. If de-Broglies equation is satisfied, then the relation between $\sin\theta$ and $\frac{1}{\sqrt{V}}$ should be linear.

There is also a particular scattering geometry inside the chamber, as shown in figure 2. α is found through

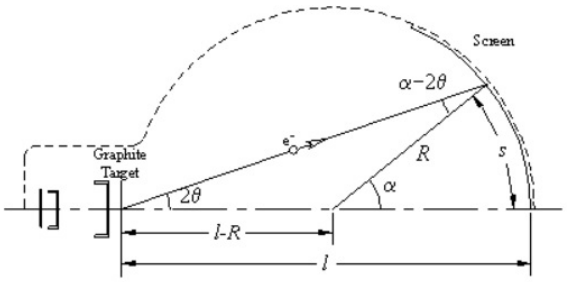

FIG. 2. Scattering Geometry Inside the Vacuum Chamber (retrieved from lab manual)

$$\alpha = \frac{s}{R}, \tag{5}$$

which leads to the following:

$$\frac{\sin(\alpha - 2\theta)}{l - R} = \frac{\sin 2\theta}{R}. \tag{6}$$

Using trigonometry, the scattering angle is determined using

$$\tan 2\theta = \frac{\sin\alpha}{\frac{l}{R} + \cos\alpha - 1} \tag{7}$$

The scattering relations can also be used to determine

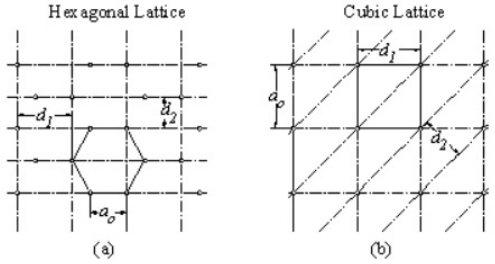

FIG. 3. Hexagonal and Cubic Lattices (retrieved from lab manual)

what type of lattice graphite is. As can be observed from figure 3, the interatomic spacing is related to the bond distance between adjacent carbon atoms in layers of the lattice by

$$d_1 = \frac{3a_0}{2} \tag{8}$$

and

$$d_2 = \frac{a_0\sqrt{3}}{2}, \tag{9}$$

where a_0 is the bond distance. These relations can be used to determine the type of lattice graphite had. From the geometry,

$$\frac{d_1}{d_2} = \sqrt{3} \tag{10}$$

indicates an hexagonal lattice, while

$$\frac{d_1}{d_2} = \sqrt{2} \tag{11}$$

indicates a cubic lattice.

Electrons are known to orbit in a uniform magnetic field. The radius of orbit can be used to calculate the charge/mass ratio of the electron. When a magnetic field is generated by Helmholtz coils, the B field near the center is approximately uniform, and its value can be calculated with the standard result from electromagnetic theory:

$$B = \frac{8\mu_0 NI}{5a\sqrt{5}}, \tag{12}$$

where N is the number of turns in a coil and a is the radius of the coil apparatus. Assuming gravity to be negligible, the force on electrons in the field is centripetal and can be found from Newtons Laws:

$$F = \frac{mv^2}{R}. \tag{13}$$

But the centripetal force is caused by the B field:

$$F = evB. \tag{14}$$

Additionally, the electrons are fired into the B field via a gun apparatus set at some potential V, and the electrons are given kinetic energy by this potential according to the following:

$$eV = \frac{mv^2}{2}. \tag{15}$$

Using these equations, the charge/mass ratio is found to be

$$\frac{e}{m} = \frac{v}{RB}. \tag{16}$$

These equations ignore relativistic effects, and since the electron speeds in this experiment are of the order of 10^7, the value of e/m will be smaller than expected due to the addition of a non-negligible Lorentz factor. But because the relativistic effects are small at these speeds, the result should only deviate slightly from the published result.

III. EXPERIMENTAL DESIGN AND PROCEDURE

A. Design

A schematic design of the 1st experiment is presented in figure 4. The design features a grounded Leybold high

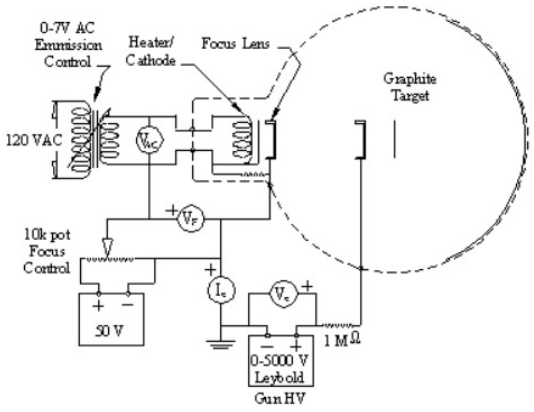

FIG. 4. Scattering Experiment Design

voltage supply connected in series with a focus control voltage supply. These are connected to a heater supply, which contains a Variac step-down transformer that generates a cathode beam. This beam is then directed through a focus lens toward a graphite crystal positioned at the entrance of a spherical glass vacuum chamber. The scattering pattern produced from the crystal is projected onto the inner surface of the chamber, where arc lengths can be measured. Three voltmeters are connected to facilitate voltage control; one is set to a 5000 V scale to monitor the high voltage supply, one is set to a 50 V scale to monitor the focus control, and one is set to a 10 V scale to monitor the heater voltage. There is also a milliammeter connected to observe the current through the filament in the heater gun.

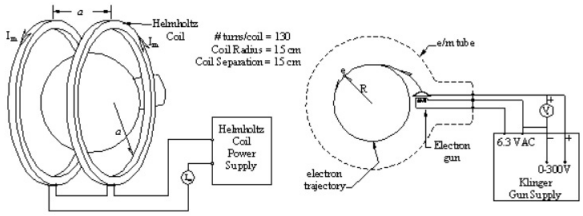

FIG. 5. Electron Orbit Experiment Design (retrieved from lab manual)

A schematic design of the 2nd experiment is presented in figure 5. An Helmholtz coil is constructed with the shown geometry. It is connected to a power supply and ammeter for current control. An electron gun apparatus is attached to the side of the coils. The gun is encased in a glass e/m tube filled with argon and is connected to a power supply, which consists of a 6.3 VAC powering the gun and a DC supply used to accelerate electrons. A standard voltmeter and ammeter are used to monitor the VAC supply and current in the Helmholtz coils, respectively. A linear HUD apparatus that measures distance on a centimeter scale is projected into the chamber where the plane of orbit will be. This HUD is used to measure the diameter of orbit of the electrons.

B. Procedure

In the first experiment, electrons were generated by the high voltage supply over the range of 1500 V to 5000 V in 200 V increments. They were funneled through the focus supply, where the focus voltage was kept between 23-26 V. The heater supply was initially set to 5.05 V but had to be varied between 3.5 V and 5.15 V over different accelerating voltages to provide for better vision of the scattering pattern. The filament current was kept between 0.125 A and 0.22 A to prevent damage to the filament. The heater produced a cathode beam that was fired into the graphite crystal, and two ring diffraction patterns were observed on the inner surface of the chamber. The diameters of these rings were recorded.

In the second experiment, an approximately uniform B-field was created in the e/m tube. Electrons were fired into the field at potentials of 200-250 V in 10 V increments. For each of these increments, the current in the coils was varied between 1.6-2.0 A in 0.1 A steps. The electrons orbited in a circle in the field. For each combination of accelerating voltage and current, the diameter of orbit was measured. Each measurement was made at 3 different orientations, and these readings were averaged for a more accurate diameter measurement.

IV. DATA ANALYSIS

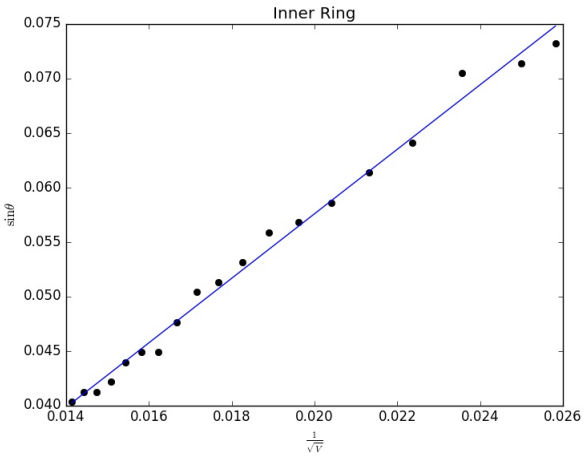

FIG. 6. Inner Ring

A table listing the scattering angles and arc lengths is given in the appendix. Figures 6 and 7 show the relationship between $\sin\theta$ and the inverse of the root voltage for both diffraction rings. Using standard regression analysis, the relation for each ring was linear with a slope of 3.0 with $R^2 = 0.99$ for the inner ring and 5.1 with $R^2 = 0.99$ for the outer ring. Using the slopes, d_1 was found to be 2.1×10^{-10} m, and d_2 was found to be 1.2×10^{-10} m. Using $a_0 = \frac{2}{3}d_1$, a_0 was found to be 1.4×10^{-10}

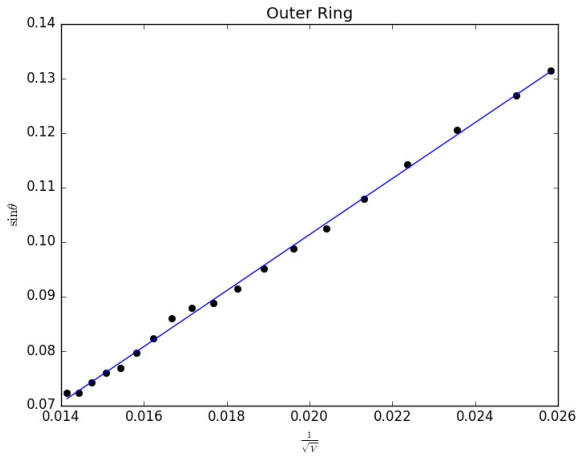

FIG. 7. Outer Ring

m. Comparing to the published value (Harrison 2012) of 1.42×10^{-10} m, there was a 2.7% error between the experimental a_0 and the published value.

A table listing d_1, d_2, and $\frac{d_1}{d_2}$ for each voltage is presented in the appendix. The average $\frac{d_1}{d_2}$ ratio was 1.8, which is closer to $\sqrt{3}$ than $\sqrt{2}$, confirming that graphite has an hexagonal lattice.

A table listing the data for the 2nd experiment is listed in the appendix. The charge/mass ratio remained remarkably consistent over all voltages and currents. The average charge to mass ratio was -1.76×10^{11} $kg/C^{-}1$. The published value is $-1.758\,820\,024 \times 10^{11}$ $kg/C^{-}1$ (CODATA), and the %error between these was 6.71×10^{-4}.

V. CONCLUSION

We have demonstrated that the electron has both wave-like and particle-like properties. Our measurement of the charge/mass ratio was very close to the published value, indicating very low experimental error for the 2nd experiment. Although results from the 1st experiment were conclusive, the 2.7% error between the calculated value and the published value indicates some error in the execution. The largest source of error in this experiment was in the measurement of the diffraction ring arc length. The edges of the rings were barely visible, and this led to imprecise measurements of the arc length. The best method of improving this experiment would be to completely darken the room in which it occurs so as to maximize vision of the ring edges.

VI. CITATIONS

CODATA. NIST Reference. URL `https://physics.nist.gov/cgi-bin/cuu/Value?esme`.

L. De Broglie. A tentative theory of light quanta. *Philosophical Magazine*, pages 446–458, 1924.

A. Einstein. Concerning an heuristic point of view toward the emission and transformation of light. *American Journal of Physics*, 33(5):367, 1965.

W. A. Harrison. *Electronic structure and the properties of solids: the physics of the chemical bond*. Courier Corporation, 2012.

J. C. Maxwell. *A dynamical theory of the electromagnetic field*. The Society, 1864.

J. J. Thomson. Xl. cathode rays. *The London, Edinburgh, and Dublin Philosophical Magazine and Journal of Science*, 44(269):293–316, 1897.

VII. APPENDIX

TABLE I. Angle Data

V	v (m/s)	s1 (cm)	a1 (rad)	th1 (rad)	s2 (cm)	a2 (rad)	th2 (rad)
1500	2.30E+07	20.00	0.31	0.073	36.00	0.561	0.132
1600	2.37E+07	19.50	0.30	0.071	34.75	0.541	0.127
1800	2.52E+07	19.25	0.30	0.071	33.00	0.514	0.121
2000	2.65E+07	17.50	0.27	0.064	31.25	0.487	0.114
2200	2.78E+07	16.75	0.26	0.061	29.50	0.460	0.108
2400	2.91E+07	16.00	0.25	0.059	28.00	0.436	0.103
2600	3.02E+07	15.50	0.24	0.057	27.00	0.421	0.099
2800	3.14E+07	15.25	0.24	0.056	26.00	0.405	0.095
3000	3.25E+07	14.50	0.23	0.053	25.00	0.389	0.092
3200	3.36E+07	14.00	0.22	0.051	24.25	0.378	0.089
3400	3.46E+07	13.75	0.21	0.050	24.00	0.374	0.088
3600	3.56E+07	13.00	0.20	0.048	23.50	0.366	0.086
3800	3.66E+07	12.25	0.19	0.045	22.50	0.350	0.082
4000	3.75E+07	12.25	0.19	0.045	21.75	0.339	0.080
4200	3.84E+07	12.00	0.19	0.044	21.00	0.327	0.077
4400	3.93E+07	11.50	0.18	0.042	20.75	0.323	0.076
4600	4.02E+07	11.25	0.18	0.041	20.25	0.315	0.074
4800	4.11E+07	11.25	0.18	0.041	19.75	0.308	0.072
5000	4.19E+07	11.00	0.17	0.040	19.75	0.308	0.072

TABLE II. Add caption

V	d1 (m)	d2 (m)	**d1/d2**
1500	2.16E-10	1.21E-10	1.79
1600	2.15E-10	1.21E-10	1.78
1800	2.05E-10	1.20E-10	1.71
2000	2.14E-10	1.20E-10	1.78
2200	2.13E-10	1.21E-10	1.76
2400	2.14E-10	1.22E-10	1.75
2600	2.12E-10	1.22E-10	1.74
2800	2.07E-10	1.22E-10	1.70
3000	2.11E-10	1.22E-10	1.72
3200	2.11E-10	1.22E-10	1.73
3400	2.09E-10	1.20E-10	1.74
3600	2.15E-10	1.19E-10	1.81
3800	2.22E-10	1.21E-10	1.83
4000	2.16E-10	1.22E-10	1.77
4200	2.15E-10	1.23E-10	1.75
4400	2.19E-10	1.22E-10	1.80
4600	2.19E-10	1.22E-10	1.80
4800	2.15E-10	1.22E-10	1.75
5000	2.15E-10	1.20E-10	1.79

TABLE III. Add caption

V	I (A)	B (Tesla)	R (m)	v (m/s)	e/m (C*kg-1)
200	1.6	1.25E-03	0.081	1.78E+07	1.76E+11
200	1.7	1.32E-03	0.076	1.77E+07	1.76E+11
200	1.8	1.40E-03	0.071	1.76E+07	1.76E+11
200	1.9	1.48E-03	0.070	1.81E+07	1.76E+11
200	2.0	1.56E-03	0.066	1.81E+07	1.76E+11
210	1.6	1.25E-03	0.085	1.86E+07	1.76E+11
210	1.7	1.32E-03	0.079	1.84E+07	1.76E+11
210	1.8	1.40E-03	0.075	1.85E+07	1.76E+11
210	1.9	1.48E-03	0.071	1.85E+07	1.76E+11
210	2.0	1.56E-03	0.068	1.85E+07	1.76E+11
220	1.6	1.25E-03	0.086	1.89E+07	1.76E+11
220	1.7	1.32E-03	0.080	1.87E+07	1.76E+11
220	1.8	1.40E-03	0.076	1.87E+07	1.76E+11
220	1.9	1.48E-03	0.073	1.89E+07	1.76E+11
220	2.0	1.56E-03	0.067	1.84E+07	1.76E+11
230	1.6	1.25E-03	0.088	1.93E+07	1.76E+11
230	1.7	1.32E-03	0.082	1.92E+07	1.76E+11
230	1.8	1.40E-03	0.078	1.93E+07	1.76E+11
230	1.9	1.48E-03	0.076	1.97E+07	1.76E+11
230	2.0	1.56E-03	0.071	1.95E+07	1.76E+11
240	1.6	1.25E-03	0.090	1.96E+07	1.76E+11
240	1.7	1.32E-03	0.085	1.97E+07	1.76E+11
240	1.8	1.40E-03	0.079	1.96E+07	1.76E+11
240	1.9	1.48E-03	0.076	1.99E+07	1.76E+11
240	2.0	1.56E-03	0.071	1.95E+07	1.76E+11
250	1.6	1.25E-03	0.092	2.01E+07	1.76E+11
250	1.7	1.32E-03	0.087	2.03E+07	1.76E+11
250	1.8	1.40E-03	0.081	2.01E+07	1.76E+11
250	1.9	1.48E-03	0.078	2.03E+07	1.76E+11
250	2.0	1.56E-03	0.073	2.00E+07	1.76E+11